UDC 577.112.6+616-006.44 doi: https://doi.org/10.15407/ubj95.02.093

CYCLIC RGD-CONTAINING PEPTIDES: *IN SILICO* EXPLORATION AGAINST BCL-X_L

A. K. OYEBAMIJI[1]✉, E. T. AKINTAYO[1,2], C. O. AKINTAYO[1,3]✉, H. O. AWORINDE[4], O. D. ADEKUNLE[1], S. A. AKINTELU[5,6]✉

[1]Industrial Chemistry Programme, Bowen University, Iwo, Osun State, Nigeria;
✉e-mail: abeloyebamiji@gmail.com;
[2]Department of Chemistry, Ekiti State University, Ado-Ekiti, Nigeria;
[3]Department of Chemistry, Federal University, Oye-Ekiti, Ekiti State, Nigeria;
✉e-mail: cecilia.akintayo@bowen.edu.ng;
[4]College of Computing and Communication Studies, Bowen University, Iwo, Nigeria;
[5]School of Chemistry and Chemical Engineering, Beijing Institute of Technology, Beijing, China;
[6]Department of Pure and Applied Chemistry, Ladoke Akintola University of Technology, Ogbomoso, Oyo State, Nigeria;
✉e-mail: akintelusundayadewale@gmail.com

Received: 08 March 2023; **Revised:** 28 April 2023; **Accepted:** 05 June 2023

*Cyclic peptides attract attention for possible applications in cancer treatment. We examined the ability of six cyclic RGD-containing peptides-based compounds to inhibit B-cell lymphoma-extra-large (Bcl-X_L) (PDB ID: 3zk6) using the in silico method. We observed that the addition of electron withdrawing group (–Cl) to cyclic RGD-containing peptides-based compound induced a radical improvement in the hydrogen bond strength with Arg139 in Bcl-X_L. Compound **F** with -9.2 kcal/mol was observed to be positioned at the best-docked site in the binding pocket of Bcl-X_L and, therefore, suggested to have greater potential anticancer ability than other studied compounds as well as the referenced compound (Doxorubicin). The ADMET properties of compound **F** and Doxorubicin were investigated and reported. Our findings may open door for the design and development of library of efficient cyclic RGD-containing peptides-based drug-like compounds as potential anti- cancer agents.*

K e y w o r d s: cyclic RGD peptides, Bcl-X_L, peptide-protein interaction, carcinogesis, in silico study, modeling.

Cancer is a serious metabolic disorder. It remains one of the top causes of mortality despite the efforts to curb the activities of cancer among human race by scientists globally [1-3]. The number of cancer cases has been observed to be rising and it has been estimated to be above eighteen million cases by 2030 [4]. According to Asma et al., 2022, the cancer-related death of several people has been attributed to four (4) kinds of cancer (Colon, breast, lung and prostate) with unidentified etiology [5]. Muhammad et al., 2023 described cancer as a malignant neoplasa as well as complicated disease with a rise in glucose secretion [6]. Several scientists also revealed that each stage of cancer relies on high manufacture of adenosine triphosphate and re-orientation of human metabolism [7].

Prostate cancer begins in human body when prostate gland develops uncontrollably. This gland can only be located in men and this makes prostate cancer peculiar to men [8]. The report shows that over twenty-five percent of men in their 40 years of age have a tendency to have this disease. This disease is considered to be type of cancer that is more common in the United States even than other types of cancer, such as skin cancer [9]. It grows slowly and other complications can lead to death of prostate cancer patients. Many researchers have developed a series of efficient drugs to combat this menace, yet death of men through prostate cancer still occur and this calls for lasting solution [10].

B-cell lymphoma-extra-large (Bcl-X_L) belongs to B-cell lymphoma-2 family. Increased production of intracellular level of Bcl-X_L is connected to growth of cancer in human being [11]. It is also responsible for growth of drug opposition by shielding cancerous cells from apoptosis [12]. Several

scientists have targeted this protein with a series of small molecules with the aim of developing efficient potential anticancer agents [13-15]. The role played by this protein in cancer initiation and progression has drawn our attention to using it as our target in order to develop more efficient anticancer drug-like molecules.

Peptides are referred to as small chains of amino acids interconnected with peptide bonds [16]. They are promising therapeutic agents such as anticancer agents etc [17]. Peptide derivatives possess enhanced selectivity as well as specificity which help them to effectively combat cancerous cells [18-20]. Report by Tsuji, 2005 showed that peptides can produce normal proteins in order to improve or prevent signal transduction [21]. They can be synthesized using mechanized approaches, and cyclic peptides have drawn the attention of several researchers due to their importance in pharmaceutical industries such as high level of selectivity, specificity, good binding affinity as well as low poisonousness [22]. Cyclic peptides are steadier and this has been reported to have enhanced their biological activities than linear peptides [23]. This work is aimed at investigating the anti-B-cell lymphoma-extra-large activity of the studied cyclic RGD-containing peptides using *in silico* approach.

Materials and Methods

Software and hardware. The studied cyclic RGD-containing peptides were optimized to get the full geometry of the studied compounds via Spartan'14 software [24]. The ability of the cyclic RGD-containing peptides to inhibit BCL-X_L was examined via density functional theory method and docking method. The softwares required for the docking study were Pymol for treating enzyme, Discovery Studio for viewing the interaction between the docked complexes, AutoDock tool for locating binding site in the studied protein and AutoDock Vina software for docking calculation.

Studied receptor. B-cell lymphoma-extra-large (Bcl-X_L) (PDB ID: 3zk6) was retrieved from protein data bank which was considered to be recognized protein database [25].

Studied pharmacophore. Six ligands were selected for this study and the selection was based on investigating the effect of electron withdrawing and electron donating groups on the parent compounds.

Preparation of B-cell lymphoma-extra-large (Bcl-X_L) (PDB ID: 3zk6). The retrieved B-cell lymphoma-extra-large (Bcl-X_L) (PDB ID: 3zk6) from the recognized protein database was subjected to discovery studio software for treatment (i.e. removal of small molecules downloaded with the protein and water molecules) [26]. The resolution, R-value free, R-value work and R-value observed for Bcl-X_L were 2.48 Å, 0.261, 0.221 and 0.222, respectively. The binding site in the studied receptor was identified, as shown in Fig. 2, using Discovery Studio software and the receptor was converted to .pdbqt using AutoDockTools-1.5.6 [27]. The calculation and analysis of site map of the studied receptor revealed the likely binding site and the figure for center (center_x = 21.072707; center_y = 49.644951 and center_z = 1.327122) as well as size of the site area (size_x = 20; size_y = 20 and size_z = 20) were reported accordingly. Also, the exhaustiveness was set to be 8 which was considered to be default. The docking calculation was executed using AutoDock Vina software so as to calculate binding affinity between the studied complexes.

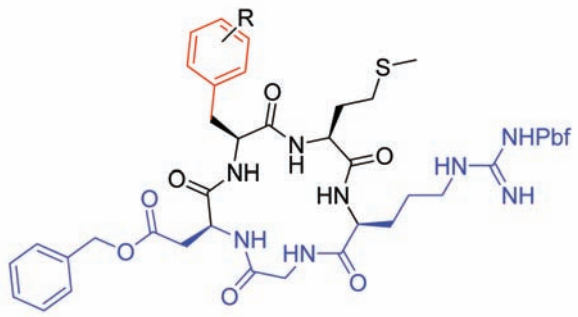

R = [A] 4-Me; [B] 4-OMe; [C] 3-Me; [D] 4-F; [E] 4-Br; [F] 4-Cl

Fig. 1. Studied RGD containing peptide

ADMET investigation. This study was executed using ADMETsar 2.0 online software [28]. The ligands with higher binding affinity were subjected to investigation, and a series of ADMET factors were considered and reported.

Molecular dynamic simulation analysis. The stability of the studied complex formed by compound **F** (compound with potential anti-prostate activity) with B-cell lymphoma-extra-large (Bcl-X_L) (PDB ID: 3zk6) was ascertained using 100,000 ps molecular dynamic simulation [29]. Also, the reference compound (Doxorubicin) with Bcl-X_L (PDB ID: 3zk6) was simulated and compared with compound **F** - Bcl-X_L complex. The selected force field for topology files was Charmm36m which was observed to be compatible with the studied complexes. The compound **F** - Bcl-X_L complex system was es-

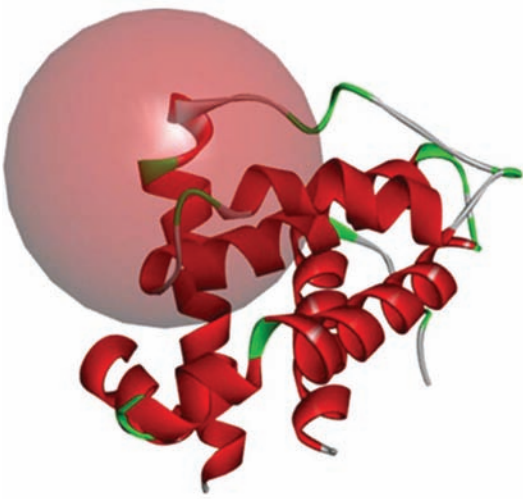

Fig. 2. 3-Dimensional structure of Bcl-X_L with identified binding site

tablished via a TIP3P water molecule together with an orthorhombic box of 10 Å on every side. In the developed system, Na^+ and Cl^- ions were added at appropriate proportion to neutralize the charged system [30]. NVT ensemble was used to execute equilibration in the system and this was followed by NPT ensemble to accomplish equilibration and minimization for another 100 nanoseconds with a 300 K as temperature and 1 bar of Pressure. Also, molecular dynamics trajectories analysis was executed via CPPTRAJ module [31].

Results and Discussion

Calculated geometries. The calculated geometries for the studied compounds were displayed in Table 1. The effect of the attached derivatives to the parent structure was investigated by observing bond length, bond angle and dihedral which were measured in Å and degree (°), respectively. It was observed that the attached derivatives have equal effect on the bond length in C7-C41 and C46-C45 but the bond length between C7 and C41 as well as C46 and C45 for compound C proved to be shorter than others; thus, 3-Me has greater effect on the length of bond between C7 and C41 as well as C46 and C45. Also, 4-F has much effect on bond length in C45-C44, C44-C43 and C43-C42 for compound D while 4-Me and 4-*o*Me have similar and highest effect in compounds A and B. The bond angle and dihedral angle were calculated and reported in Table 1.

Calculated electronic properties for studied compounds. The descriptors obtained from optimized studied peptides are presented in Table 2. The

Table 1. Selected geometry parameters obtained by B3LYP/5-31G for the studied molecules*

	A	B	C	D	E	F
C7-C41	1.515 Å	1.515 Å	1.514 Å	1.515 Å	1.515 Å	1.515 Å
C46-C45	1.397 Å	1.397 Å	1.395 Å	1.396 Å	1.397 Å	1.398 Å
C45-C44	1.398 Å	1.395 Å	1.394 Å	1.388 Å	1.392 Å	1.392 Å
C44-C43	1.398 Å	1.393 Å	1.398 Å	1.388 Å	1.392 Å	1.392 Å
C43-C42	1.397 Å	1.400 Å	1.401 Å	1.395 Å	1.397 Å	1.397 Å
C42-C41	1.403 Å	1.403 Å	1.405 Å	1.406 Å	1.404 Å	1.404 Å
C41, C46, C45	120.56°	120.37°	120.38°	120.45°	120.56°	120.53°
C46, C45, C44	120.64°	120.90°	120.23°	119.70°	119.87o	119.94°
C45, C44, C43	118.97°	119.09°	120.34°	120.85°	120.37°	120.29°
C44, C43, C42	120.44°	120.18°	119.12°	119.61°	119.73°	119.81°
C43, C42, C41	120.75°	120.93°	121.00°	120.55°	120.68°	120.64°
C42, C41, C46	118.59°	118.48°	118.87°	118.81°	118.76°	118.76°
C41, C46, C45, C44	-1.36°	-0.75°	-0.77°	-0.93°	-0.81°	-0.81°
C45, C44, C43, C42	-0.55°	0.82°	1.65°	0.56°	0.51°	-0.48°
C44, C43, C42, C41	1.45°	0.90°	-0.07°	0.53°	0.85°	0.84°
C43, C42, C41, C46	-2.25°	-2.51°	-1.89°	-1.78°	-2.15°	-2.10°
C42, C41, C46, C45	2.20°	2.43°	2.31°	1.97°	2.13°	2.08°

E_{HOMO} (highest occupied molecular orbital energy) and E_{LUMO} (lowest unoccupied molecular orbital energy) play a crucial responsibility calculating the release and receiving of electron in any compound. Also, both descriptors possess the ability to reveal the level of reactivity, biological strength and stability of the studied compound [32]. Cao et al., 2005, reported that efficient donating strength of any molecule is a function of the highest E_{HOMO}, while effective ability to receive charge from nearby compound is a function of lowest E_{LUMO} value [33]. In this work, compounds **E** and **F** proved to have highest strength to react well than other studied compounds, while compound **E** with lowest E_{LUMO} value (-1.00) also proved to have tendency to react well.

The calculated band-gap originated from E_{LUMO} - E_{HOMO}. The closer the reacting compounds to each other, the chemically active the reacting compound is and this could also be regarded as soft molecule; thus, compound **E** with -1.00 eV have the greatest tendency to chemically react than other studied compounds (Table 2). The decreasing order of the calculated band gap is as follows: A = B > D > C > F > E revealing the increasing order of the chemical reactivity of the studied compounds.

Table 2. Calculated reactivity descriptors from optimized 3D structures of studied peptides

	E_{HOMO} (eV)	E_{LUMO} (eV)	BG (eV)
A	-6.08	-0.74	5.34
B	-6.09	-0.75	5.34
C	-6.03	-0.85	5.18
D	-6.05	-0.85	5.20
E	-5.77	-1.00	4.77
F	-5.77	-0.98	4.79

Calculated molecular docking study. In this work, the studied compounds **A-F** were docked into the active site of B-cell lymphoma-extra-large (Bcl-X_L) (PDB ID: 3zk6) to investigate the intermolecular interactions between studied complexes. Also, the prospective binding configurations that back these studied peptides' inhibitory abilities were observed. In each of the docking studies, nine con-

Table 3. Calculated binding affinity and residues involved in the interaction

	Binding Affinity (kcal/mol)	Residues involved in the interactions	Types of Non-bonding interaction
A	-9.0	Phe97, Tyr101, Val141, Phe105, Arg139, Ala142, Leu108	Conventional Hydrogen Bond, Pi-Pi Stacked, Alkyl, Pi-Alkyl
B	-8.6	Tyr101, Phe97, Val141, Arg139, Ala142, Leu130, Phe105	Conventional Hydrogen Bond, Pi-Pi Stacked, Alkyl, Pi-Alkyl
C	-8.0	Ala104, Phe105, Phe97, Leu130, Ala142, Asn136, Arg139, Tyr195, Val141, Ala93,	Conventional Hydrogen Bond, Unfavourable positive-positive, Unfavourable Donor-Donor, Pi-Cation, Pi-Donor Hydrogen Bond, Pi-Pi Stacked, Alkyl, Pi-Alkyl
D	-8.1	Arg139, Phe105, Leu130, Phe97, Ala142, Tyr195, Val141, Ala93, Tyr101	Conventional Hydrogen bond, Halogen (Fluorine), Pi-Donor Hydrogen Bond, Pi-Pi Stacked, Alkyl, Pi-Alky
E	-8.9	Arg139, Phe105, Phe97, Tyr101	Pi-Pi Stacked, Conventional Hydrogen Bond, Pi-Pi T-shaped, Pi-Alkyl
F	-9.2	Leu108, Phe105, Asp133, Arg102, Phe97, Ala142, Val141, Leu130, Arg139, Ala93, Tyr195	Conventional Hydrogen Bond, Attractive Charge, Unfavourable Donor-Donor, Pi-Pi T-shaped, Alkyl, Pi-Alkyl
Doxorubicin	-7.8	–	–

figurations were observed and the pose with lowest binding affinity value was selected. As shown in Table 3, the binding score for the docked complexes were -9.0, -8.6, -8.0, -8.1, -8.9 and -9.2 kcal/mol for compounds **A**-**F**, respectively. The calculated binding affinity revealed that all the studied compounds were located at the best-docked site in the active site of B-cell lymphoma-extra-large (Bcl-X_L) (PDB ID: 3zk6) when compared to binding affinity for the referenced compound (Doxorubicin) with -7.8 kcal/mol. According to report by Oyebamiji et al., 2022, the lower the calculated binding affinity, the more strength to the target; therefore, compound **F** has potential greater strength to inhibit B-cell lymphoma-extra-large (Bcl-X_L) (PDB ID: 3zk6) thereby down-regulate prostate cancer [34]. More so, among the studied compounds, compound **F** proved to be positioned at best docked site in the active site of the studied receptor (Fig. 3 and 4).

Furthermore, the amino acid residue found in the pocket site of B-cell lymphoma-extra-large (Bcl-X_L) (PDB ID: 3zk6) was observed to play crucial role in establishing non-bonding interaction with the studied compounds. Compound **F** forms attractive charge with Asp133; conventional hydrogen bond with Arg 139; unfavorable donor-donor with Arg139; Pi-Pi T-shaped with Phe105 and Phe97; Alkyl and pi-Alkyl with Val-141, Ala93, Tyr195, Leu130, Leu 108, Ala142 and Arg102. The non-bonding interactions formed with other studied compounds were reported in Table 3.

Molecular dynamic simulation analysis

Root mean square deviation analysis. The root mean square deviation (RMSD) of compound **F** (compound with best binding affinity from docking study) was used to quantify the amount of nonconformity from the original structure and the steadiness of the studied complexes all through 100,000 ps (100 ns) simulation time. The RMSD revealed that compound **F** reacted well with Bcl-X_L (PDB ID: 3zk6) and it proved that it has greater ability to inhibit the studied receptor than the referenced compound, as shown in Fig. 5.

Calculated binding energy. Table 4 revealed the calculated binding energy components which was measured in kcal/mol for compound **F** and

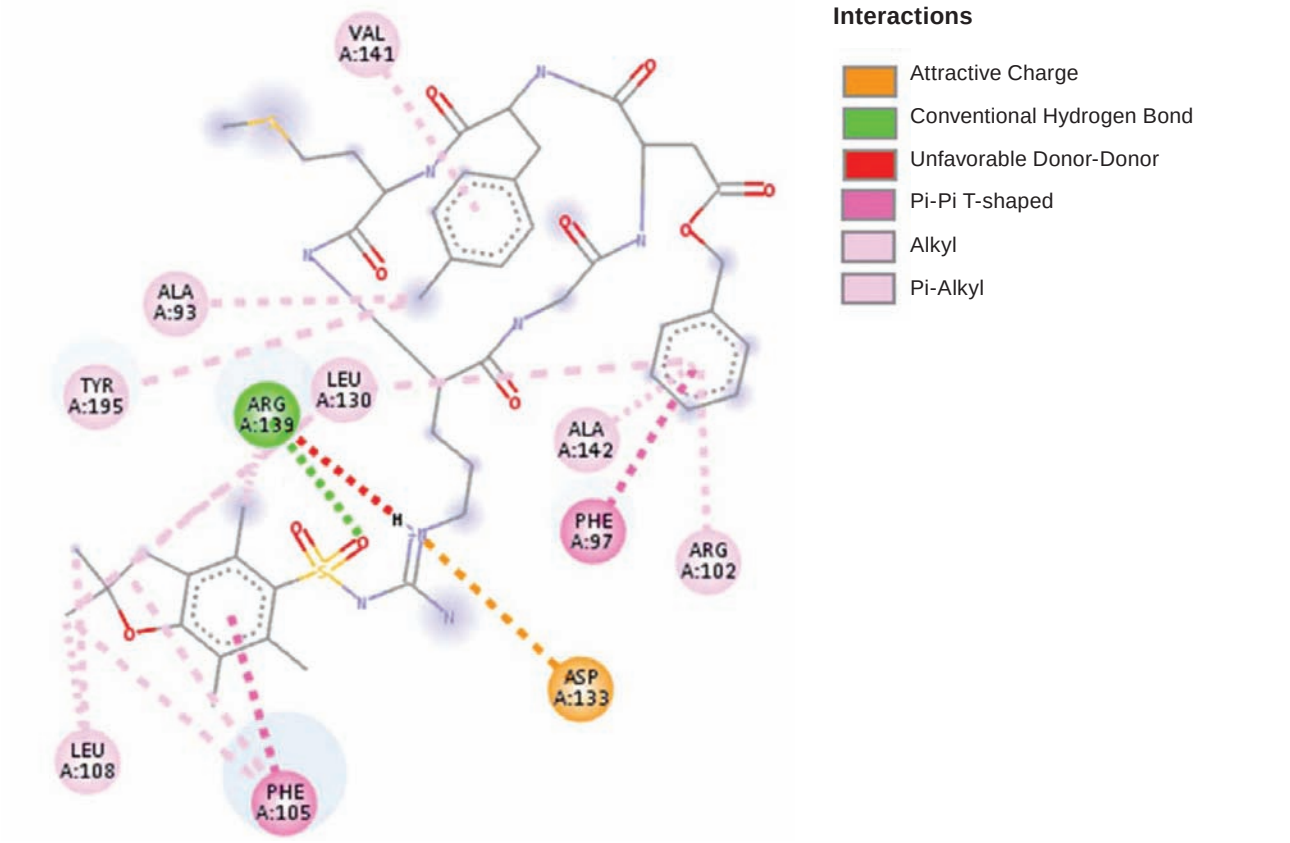

Fig. 3. Two dimensional (2D) binding configuration of compound F in the binding pocket of Bcl-X_L (PDB ID: 3zk6)

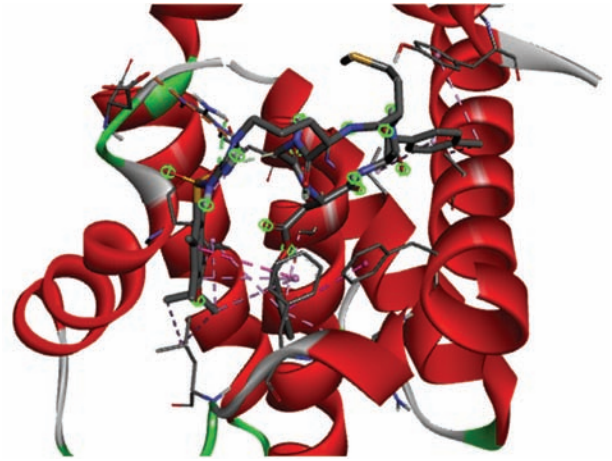

*Fig. 4. Three dimensional (3D) binding configuration of compound **F** in binding pocket of Bcl-X_L (PDB ID: 3zk6)*

referenced compound (Doxorubicin) against B-cell lymphoma-extra-large (Bcl-X_L) (PDB ID: 3zk6) via molecular dynamic simulation study. The binding energy calculated for compound **F** - Bcl-X_L complex revealed its ability to inhibit B-cell lymphoma-extra-large (Bcl-X_L) than Doxorubicin (reference compound). The binding energy for compound **F** - Bcl-X_L and reference compound - Bcl-X_L complexes were 10.35 ± 1.84 and 12.26 ± 1.08 kcal/mol, respectively. Other calculated free energy for compound **F** - Bcl-X_L were van der Waal energy (ΔE_{vdw}) (-60.65 ± 0.61 kcal/mol), electrostatic energy (ΔE_{ele}) (-133.39 ± 3.24 kcal/mol), gas-phase molecular mechanics free energy (ΔG_{gas}) (-194.04 ± 3.49 kcal/mol) and polar solvation energy (ΔG_{sol}) (204.38 ± 4.64 kcal/mol) while other calculated free energy for reference compound (Doxorubicin) - Bcl-X_L were -41.04 ± 0.7 kcal/mol for van der Waal energy (ΔE_{vdw}), 10.3 ± 2.76 kcal/mol for electrostatic energy (ΔE_{ele}), -2.65 ± 0.44 kcal/mol for gas-phase molecular mechanics free energy (ΔG_{gas}) and -51.33 ± 0.65 kcal/mol for polar solvation energy (ΔG_{sol}). As shown in Table 4, van der Waal energy, electrostatic energy and gas-phase molecular mechanics free energy were favorable towards binding of compound **F** to the active site of B-cell lymphoma-extra-large (Bcl-X_L) (PDB ID: 3zk6) (Fig. 6).

ADMET Evaluation

In drug design and discovery, the *in silico* approach to develop the drug-like features is very time and cost-effective before the synthesis of targeted compounds. Blood brain barrier value for compound **F** was greater than -1 which revealed that the compound has the ability to be fairly distributed through

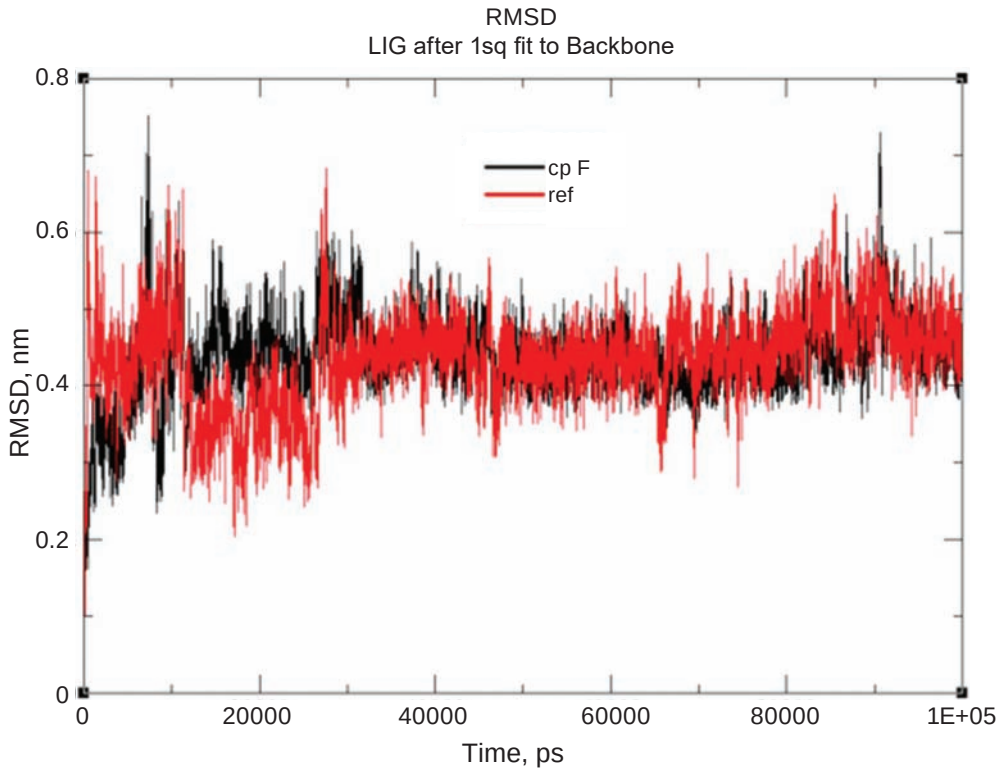

Fig. 5. RMSD of Comp F-Bcl(X_L) and Ref-protein complexes during 100 ns MD trajectories

*Table 4. Calculated binding energy components measured in kcal/mol for Comp **F** - Bcl-X_L and Ref-protein*

Complexes	Binding energy components, kcal/mol				
	ΔE_{vdw}	ΔE_{ele}	ΔG_{gas}	ΔG_{sol}	ΔG_{bind}
Comp **F** - Bcl- X_L	-60.65 ± 0.61	-133.39 ± 3.24	-194.04 ± 3.49	204.38 ± 4.64	10.35 ± 1.84
REF-protein	-41.04 ± 0.70	10.30 ± 2.76	-2.65 ± 0.44	-51.33 ± 0.65	12.26 ± 1.08

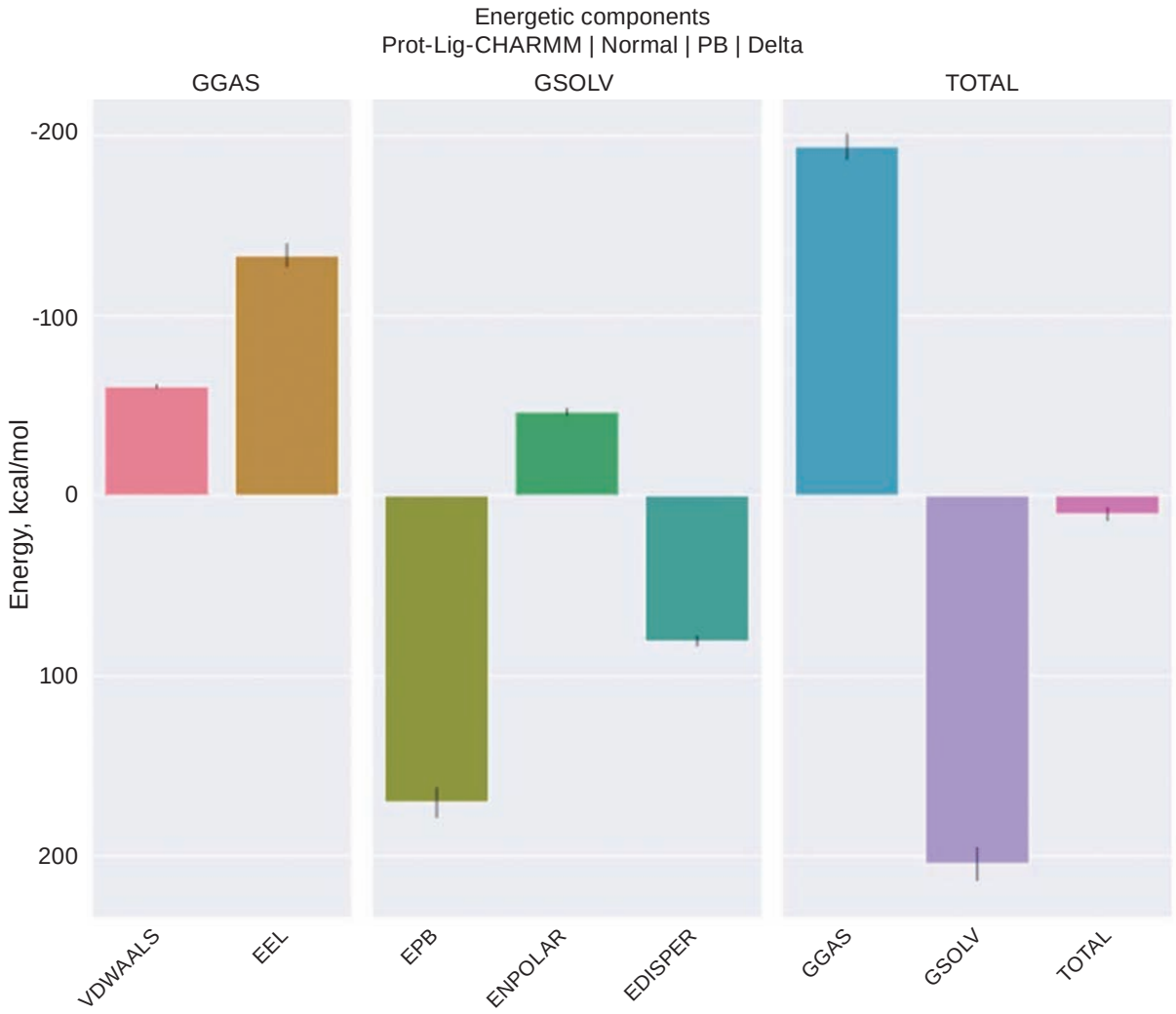

Fig. 6. Chart for calculated binding energy components

the brain. This was well correlated with the BBB value calculated for the referenced compound. As shown in Tables 4 and 5, the calculated value for human intestinal absorption for compound **F** and the referenced compound were 0.9652 and 0.8092, respectively. This proved to be above the threshold value of 30% and this showed that both compound **F** and doxorubicin have high human intestinal absorption features. As shown in Table 4, compound **F** was observed to be non-substrate to CYP450 2C9 Substrate, CYP450 2D6 Substrate and was observed to be substrate to CYP450 3A4 Substrate and these properties agreed well with the properties observed for referenced compound. More so, compound **F** was non-inhibitor to CYP450 1A2, CYP450 2C9, CYP450 2D6 and CYP450 2C19, but it only has the ability to inhibit CYP450 3A4. The selected compound was observed to be non-carcinogenic, non-

*Table 4. ADMET features for compound **F** (compound with highest binding affinity)*

ADMET Predicted Profile – Classification		
Model	Result	Probability
Absorption		
Blood-Brain Barrier	BBB-	0.8667
Human Intestinal Absorption	HIA+	0.9652
Caco-2 Permeability	Caco2-	0.6709
P-glycoprotein Substrate	Substrate	0.9069
P-glycoprotein Inhibitor	Inhibitor	0.5239
	Non-inhibitor	0.7775
Renal Organic Cation Transporter	Non-inhibitor	0.7290
Distribution		
Subcellular localization	Lysosome	0.4864
Metabolism		
CYP450 2C9 Substrate	Non-substrate	0.5915
CYP450 2D6 Substrate	Non-substrate	0.7832
CYP450 3A4 Substrate	Substrate	0.6931
CYP450 1A2 Inhibitor	Non-inhibitor	0.7147
CYP450 2C9 Inhibitor	Non-inhibitor	0.5867
CYP450 2D6 Inhibitor	Non-inhibitor	0.8513
CYP450 2C19 Inhibitor	Non-inhibitor	0.5904
CYP450 3A4 Inhibitor	Inhibitor	0.8571
CYP Inhibitory Promiscuity	High CYP Inhibitory Promiscuity	0.5952
Toxicity		
Human Ether-a-go-go-Related Gene Inhibition	Weak inhibitor	0.8309
	Inhibitor	0.5978
AMES Toxicity	Non AMES toxic	0.5854
Carcinogens	Non-carcinogens	0.6548
Fish Toxicity	High FHMT	0.9990
Tetrahymena Pyriformis Toxicity	High TPT	0.9770
Honey Bee Toxicity	Low HBT	0.6606
Biodegradation	Not ready biodegradable	1.0000
Acute Oral Toxicity	III	0.5599
Carcinogenicity (Three-class)	Non-required	0.5712
ADMET Predicted Profile – Regression		
Model	Value	Unit
Absorption		
Aqueous solubility	-3.9321	LogS
Caco-2 Permeability	0.0007	LogPapp, cm/s
Toxicity		
Rat Acute Toxicity	2.5817	LD50, mol/kg
Fish Toxicity	1.3470	pLC50, mg/l
Tetrahymena Pyriformis Toxicity	0.5693	pIGC50, ug/l

Table 5. ADMET features for doxorubicin (Referenced Compound)

ADMET Predicted Profile – Classification		
Model	Result	Probability
Absorption		
Blood-Brain Barrier	BBB-	0.9951
Human Intestinal Absorption	HIA-	0.8092
Caco-2 Permeability	Caco2-	0.7990
P-glycoprotein Substrate	Substrate	0.7861
P-glycoprotein Inhibitor	Non-inhibitor	0.8782
	Non-inhibitor	0.8382
Renal Organic Cation Transporter	Non-inhibitor	0.9053
Distribution		
Subcellular localization	Nucleus	0.8460
Metabolism		
CYP450 2C9 Substrate	Non-substrate	0.8042
CYP450 2D6 Substrate	Non-substrate	0.9116
CYP450 3A4 Substrate	Substrate	0.5888
CYP450 1A2 Inhibitor	Non-inhibitor	0.9045
CYP450 2C9 Inhibitor	Non-inhibitor	0.9209
CYP450 2D6 Inhibitor	Non-inhibitor	0.9231
CYP450 2C19 Inhibitor	Non-inhibitor	0.9025
CYP450 3A4 Inhibitor	Non-inhibitor	0.8310
CYP Inhibitory Promiscuity	Low CYP Inhibitory Promiscuity	0.8911
Excretion		
Toxicity		
Human Ether-a-go-go-Related Gene Inhibition	Weak inhibitor	0.9752
	Non-inhibitor	0.7195
AMES Toxicity	AMES toxic	0.9198
Carcinogens	Non-carcinogens	0.9534
Fish Toxicity	High FHMT	0.8704
Tetrahymena Pyriformis Toxicity	High TPT	0.9877
Honey Bee Toxicity	Low HBT	0.5612
Biodegradation	Not ready biodegradable	0.9672
Acute Oral Toxicity	III	0.7766
Carcinogenicity (Three-class)	Non-required	0.6246

ames toxic and not readily biodegradable. Other calculated ADMET features for compound **F** and the standard are shown in Tables 4 and 5.

Conclusion. Six cyclic RGD-containing peptides were explored using *in silico* approach. Series of descriptors that revealed the properties of the studied compounds were obtained via 6-31G* as basis set using Spartan'14 software. The descriptors obtained from the optimized peptides revealed that the studied peptides have potential anti-prostate cancer capacity. Also, the studied peptides were docked into the binding pocket of the studied receptor and it was observed that all the studied peptides proved to be active and possess greater ability to inhibit Bcl-X_L (PDB ID: 3zk6) than the doxorubicin (Referenced compound). Compound **F** with the highest binding

Table 5. (Continuation)

ADMET Predicted Profile – Regression		
Model	Value	Unit
Absorption		
Aqueous solubility	-2.7191	LogS
Caco-2 Permeability	-0.5350	LogPapp, cm/s
Distribution		
Metabolism		
Excretion		
Toxicity		
Rat Acute Toxicity	2.6644	LD50, mol/kg
Fish Toxicity	1.3320	pLC50, mg/l
Tetrahymena Pyriformis Toxicity	0.3955	pIGC50, ug/l

affinity and the binding score of -9.2 kcal/mol proved to be potent to inhibit B-cell lymphoma-extra-large (Bcl-X_L) than other studied compounds. The ADMET features calculated for compound **F** and Doxorubicin (ref drug) revealed that compound **F** has potential characteristic to act as potential drug-like compound with anti-prostate ability.

Acknowledgements. We are grateful to the Industrial Chemistry Programme, Bowen University, for the computational resources and Mrs E.T. Oyebamiji, as well as Miss Priscilla F. Oyebamiji, for the assistance in the course of this study.

Conflict of interest. The authors have completed the Unified Conflicts of Interest form at http://ukr-biochemjournal.org/wp-content/uploads/2018/12/coi_disclosure.pdf and declare no conflict of interest.

Funding. We are grateful to Bowen University Research Grant Programme for the grant (Grant No: BURG/2023/009).

ЦИКЛІЧНІ RGD-ВМІСНІ ПЕПТИДИ: *IN SILICO* ДОСЛІДЖЕННЯ ПРОТИ BCL-X_L

A. K. Oyebamiji[1]✉, *E. T. Akintayo*[1,2], *C. O. Akintayo*[1,3]✉, *H. O. Aworinde*[4], *O. D. Adekunle*[1], *S. A. Akintelu*[5,6]✉

[1]Industrial Chemistry Programme, Bowen University, Iwo, Osun State, Nigeria;
✉e-mail: abeloyebamiji@gmail.com;
[2]Department of Chemistry, Ekiti State University, Ado-Ekiti, Nigeria;
[3]Department of Chemistry, Federal University, Oye-Ekiti, Ekiti State, Nigeria;
✉e-mail: cecilia.akintayo@bowen.edu.ng;
[4]College of Computing and Communication Studies, Bowen University, Iwo, Nigeria;
[5]School of Chemistry and Chemical Engineering, Beijing Institute of Technology, Beijing, China;
[6]Department of Pure and Applied Chemistry, Ladoke Akintola University of Technology, Ogbomoso, Oyo State, Nigeria;
✉e-mail: akintelusundayadewale@gmail.com

Циклічні пептиди привертають увагу можливим застосуванням у лікуванні раку. Ми перевірили здатність шести циклічних RGD-вмісних пептидів інгібувати надвелику В-клітинну лімфому (Bcl-X_L) (PDB ID: 3zk6) з використанням методу *in silic*o. Додавання електроноакцепторної групи (–Cl) до сполуки на основі циклічних RGD-вмісних пептидів спричиняло радикальне покращення міцності водневого зв'язку з Arg139 у Bcl-X_L з Arg139. Було виявлено, що сполука **F** з -9,2 ккал/моль розташована в найкращому місці стикування в кишені зв'язування Bcl-X_L і має більшу потенційну протиракову здатність, ніж інші досліджувані сполуки, а також контрольна сполука (доксорубіцин). Властивості сполуки **F** і доксорубіцину були досліджені за допомогою програми ADMET. Наші результати відкривають можливості для проектування та розробки бібліотеки ефективних циклічних RGD-вмісних пептидів на основі лікарських речовин як потенційних протиракових агентів.

Ключові слова: циклічні RGD пептиди, Bcl-X_L, пептид-протеїнова взаємодія, канцерогенез, *in silico* дослідження, моделювання.

References

1. Javed I, Banzeer AA, Tariq M, Sobia K, Barkat A, Sayed SA, Ali KT. Plant-derived anticancer agents: A green anticancer approach. *Asian Pac J Trop Biomed*. 2017; (12): 1129-1150.
2. He L, Gu J, Lim LY, Yuan ZX, Mo J. Nanomedicine-Mediated Therapies to Target Breast Cancer Stem Cells. *Front Pharmacol*. 2016; 7: 313.
3. Qin W, Huang G, Chen Z, Zhang Y. Nanomaterials in Targeting Cancer Stem Cells for Cancer Therapy. *Front Pharmacol*. 2017; 8: 1.
4. Siegel RL, Miller KD, Jemal A. Cancer statistics, 2016. *CA Cancer J Clin*. 2016; 66(1): 7-30.
5. Asma ST, Acaroz U, Imre K, Morar A, Shah SRA, Hussain SZ, Arslan-Acaroz D, Demirbas H, Hajrulai-Musliu Z, Istanbullugil FR, Soleimanzadeh A, Morozov D, Zhu K, Herman V, Ayad A, Athanassiou C, Ince S. Natural Products/Bioactive Compounds as a Source of Anticancer Drugs. *Cancers (Basel).* 2022; 14(24): 6203.
6. Muhammad SNH, Safuwan NAM, Yaacob NS, Fauzi AN. Regulatory Mechanism on Anti-Glycolytic and Anti-Metastatic Activities Induced by Strobilanthes crispus in Breast Cancer, In Vitro. *Pharmaceuticals*. 2023; 16(2): 153.
7. De la Cruz-López KG, Castro-Muñoz LJ, Reyes-Hernández DO, García-Carrancá A, Manzo-Merino J. Lactate in the Regulation of Tumor Microenvironment and Therapeutic Approaches. *Front Oncol*. 2019; 9: 1143.
8. Merriel SWD, Funston G, Hamilton W. Prostate Cancer in Primary Care. *Adv Ther*. 2018; 35(9): 1285-1294.
9. Zelefsky MJ, Morris MJ, Eastham JA. Chapter 70: Cancer of the Prostate. In: DeVita VT, Lawrence TS, Rosenberg SA, eds. DeVita, Hellman, and Rosenberg's Cancer: Principles and Practice of Oncology. 11th ed. Philadelphia, Pa: Lippincott Williams & Wilkins; 2019.
10. Bokhorst LP, Bangma CH, van Leenders GJLH, Lous JJ, Moss SM, Schröder FH, Roobol MJ. Prostate-specific antigen-based prostate cancer screening: reduction of prostate cancer mortality after correction for nonattendance and

contamination in the Rotterdam section of the European Randomized Study of Screening for Prostate Cancer. *Eur Urol.* 2014; 65(2): 329-336.
11. Li M, Wang D, He J, Chen L, Li H. Bcl-X_L: A multifunctional anti-apoptotic protein. *Pharmacol Res.* 2020; 151: 104547.
12. Hanahan D, Weinberg RA. Hallmarks of cancer: the next generation. *Cell.* 2011; 144(5): 646-674.
13. Ashkenazi A, Fairbrother WJ, Leverson JD, Souers AJ. From basic apoptosis discoveries to advanced selective BCL-2 family inhibitors. *Nat Rev Drug Discov.* 2017; 16(4): 273-284.
14. Opferman JT. Attacking cancer's Achilles heel: antagonism of anti-apoptotic BCL-2 family members. *FEBS J.* 2016; 283(14): 2661-2675.
15. Garner TP, Lopez A, Reyna DE, Spitz AZ, Gavathiotis E. Progress in targeting the BCL-2 family of proteins. *Curr Opin Chem Biol.* 2017; 39: 133-142.
16. Chavda VP, Solanki HK, Davidson M, Apostolopoulos V, Bojarska J. Peptide-Drug Conjugates: A New Hope for Cancer Management. *Molecules.* 2022; 27(21): 7232.
17. Apostolopoulos V, Bojarska J, Chai TT, Elnagdy S, Kaczmarek K, Matsoukas J, New R, Parang K, Lopez OP, Parhiz H, Perera CO, Pickholz M, Remko M, Saviano M, Skwarczynski M, Tang Y, Wolf WM, Yoshiya T, Zabrocki J, Zielenkiewicz P, AlKhazindar M, Barriga V, Kelaidonis K, Sarasia EM, Toth I. A Global Review on Short Peptides: Frontiers and Perspectives. *Molecules.* 2021; 26(2): 430.
18. Apostolopoulos V, Bojarska J, Feehan J, Matsoukas J, Wolf W. Smart therapies against global pandemics: A potential of short peptides. *Front Pharmacol.* 2022;13:914467.
19. Apostolopoulos V, Bojarska J, Chai TT, Feehan J, Kaczmarek K, Matsoukas JM, Paredes-Lopez O, Saviano M, Skwarczynski M, Smith-Carpenter J, Venanzi M, Wolf WM, Zielenkiewicz P, Ziora ZM. New Advances in Short Peptides: Looking Forward. *Molecules.* 2022; 27(11): 3635.
20. Bojarska J, Mieczkowski A, Ziora ZM, Skwarczynski M, Toth I, Shalash AO, Parang K, El-Mowafi SA, Mohammed EHM, Elnagdy S, AlKhazindar M, Wolf WM. Cyclic Dipeptides: The Biological and Structural Landscape with Special Focus on the Anti-Cancer Proline-Based Scaffold. *Biomolecules.* 2021; 11(10): 1515.
21. Tsuji A. Small molecular drug transfer across the blood-brain barrier via carrier-mediated transport systems. *NeuroRx.* 2005; 2(1): 54-62.
22. Ramadhani D, Maharani R, Gazzali AM, Muchtaridi M. Cyclic Peptides for the Treatment of Cancers: A Review. *Molecules.* 2022; 27(14): 4428.
23. Qian Z, Rhodes CA, McCroskey LC, Wen J, Appiah-Kubi G, Wang DJ, Guttridge DC, Pei D. Enhancing the Cell Permeability and Metabolic Stability of Peptidyl Drugs by Reversible Bicyclization. *Angew Chem Int Ed Engl.* 2017; 56(6): 1525-1529.
24. Semire B, Oyebamiji AK, Odunola OA. Tailoring of energy levels in (2Z)-2-cyano-2-[2-[(E)-2-[2-[(E)-2-(p-tolyl)vinyl]thieno[3,2-b]thiophen-5-yl] vinyl]pyran-4-ylidene]acetic acid derivatives via conjugate bridge and fluorination of acceptor units for effective D–π–A dye-sensitized solar cells: DFT–TDDFT approach. *Res Chem Intermediates.* 2017; 43(3): 1863-1879.
25. Lessene G, Czabotar PE, Sleebs BE, Zobel K, Lowes KN, Adams JM, Baell JB, Colman PM, Deshayes K, Fairbrother WJ, Flygare JA, Gibbons P, Kersten WJA, Kulasegaram S, Moss RM, Parisot JP, Smith BJ, Street IP, Yang H, Huang DCS, Watson KG. Structure-guided design of a selective BCL-X(L) inhibitor. *Nat Chem Biol.* 2013; 9(6): 390-397.
26. Erazua EA., Oyebamiji AK, Akintelu SA, Adewole PD, Adelakun A, Adeleke BB. Quantitative Structure-Activity relationship, Molecular Docking and ADMET Screening of Tetrahydroquinoline Derivatives as Anti-Small Cell Lung Cancer Agents. *Eclética Química.* 2023; 48(1): 55-71.
27. Waziri I, Kelani MT, Oyedeji-Amusa MO, Oyebamiji AK, Coetzee LCC, Adeyinka AS, Muller AJ. Synthesis and computational investigation of N,N-dimethyl-4-[(Z)-(phenylimino)methyl]aniline derivatives: Biological and quantitative structural activity relationship studies. *J Mol Struct.* 2023; 1276: 134756.
28. Belay Y, Muller A, Ndinteh DT, Oyebamiji AK, Adeyinka AS, Fonkui TY. Synthesis, antibacterial activities, cytotoxicity, and molecular doking studies of Salicyledene derivatives. *J Mol Struct.* 2023; 1275: 134623.
29. Çevik UA, Celik I, Işık A, Pillai RR, Tallei TE, Yadav R, Özkay Y, Kaplancıklı ZA. Synthesis,

molecular modeling, quantum mechanical calculations and ADME estimation studies of benzimidazole-oxadiazole derivatives as potent antifungal agents. *J Mol Struct.* 2022; 1252: 132095.

30. Radwan HA, Ahmad I, Othman IMM, Gad-Elkareem MAM, Patel H, Aouadi K, Snoussi M, Kadri A. Design, synthesis, *in vitro* anticancer and antimicrobial evaluation, SAR analysis, molecular docking and dynamic simulation of new pyrazoles, triazoles and pyridazines based isoxazolee. *J Mol Struct.* 2022; 1264: 133312.
31. Roe DR, Cheatham TE 3rd. PTRAJ and CPPTRAJ: Software for Processing and Analysis of Molecular Dynamics Trajectory Data. *J Chem Theory Comput.* 2013; 9(7): 3084-3095.
32. Świsłocka R, Regulska E, Karpińska J, Świderski G, Lewandowski W. Molecular Structure and Antioxidant Properties of Alkali Metal Salts of Rosmarinic Acid. Experimental and DFT Studies. *Molecules.* 2019; 24(14): 2645.
33. Cao H, Cheng WX, Li C, Pan X., Xie XG, Li TH. DFT study on the antioxidant activity of rosmarinic acid. *J Mol Struct Theochem.* 2005; 719(1-3): 177-183.
34. Oyebamiji AK, Akintayo ET, Semire B, Odelade KA, Adetuyi BO, Amin H, Batiha GE. Insilico Investigation on Isatin (1H-indole-2,3-dione) Derivatives as Potential Anti-tumor Necrosis Factor-Alpha. *Trop J Nat Prod Res.* 2022; 6(11): 1870-1875.